

Wei Guo, Qiang Jia, Ruiting Li and Weidong Li*

The Superplastic Deformation Behavior and Phase Evolution of Ti-6Al-4V Alloy at Constant Tensile Velocity

DOI 10.1515/htmp-2015-0205

Received September 20, 2015; accepted January 16, 2016

Abstract: The superplastic tensile behaviors of Ti-6Al-4V (TC4) titanium alloy were tested at temperature ranges from 850 °C to 950 °C and tensile velocities in the range of 0.3–6.0 mm/min. The microstructures of the specimen under various deformation parameters were evaluated by scanning electron microscope (SEM) and transmission electron micrograph (TEM). The results indicate that the maximum tensile force decreases with the increase of temperature and the decrease of tensile velocity. The optimum tensile elongation of 1120.5 % is attained at 900 °C and 0.6 mm/min. α and β phase grain sizes increase with the increase of temperature and the decrease of tensile velocity. β phase volume fraction plays an important role in superplasticity, and the best elongation is attained under the condition of $\sim 7.0 \mu\text{m}$ α phase and $\sim 4.0 \mu\text{m}$ β phase and β phase volume fraction is about 31%. High deformation velocity leads to finer grains and results in larger tensile force.

Keywords: Ti-6Al-4V, superplastic deformation, microstructure, elongation, phase transformation

PACS® (2010). 62.20.Fe

Introduction

Due to its lots of merits, such as low density, attractive specific strength, high strength and excellent corrosion resistance, Ti-6Al-4V titanium alloy has been widely used in many industries. However, because of its low plasticity and formability at room temperature, the use of Ti-6Al-4V titanium alloy was limited once upon a time. Fortunately, studies have found that many commercial titanium alloys with stable equiaxed fine grain microstructure, such as Ti-6Al-4V titanium alloy, possess

superplasticity characteristic, and the elongation of Ti-6Al-4V alloy can even exceed 1,000 % [1]. Up to now, many components of airframe structures are produced by superplastic forming of Ti-6Al-4V alloy [2], and its commercial applications are expected to increase.

In decades of years, considerable efforts have been devoted to investigate the superplastic behaviors, demonstrate superplastic properties and verify superplastic deformation mechanisms of titanium alloy [3–8]. For example, it has been found that Ti-6Al-4V shows superplastic behaviors under the temperature between 750 °C and 950 °C at strain rates between 10^{-4} s^{-1} and $5 \times 10^{-3} \text{ s}^{-1}$ [3, 5]. As an $\alpha + \beta$ phase alloy, Ti-6Al-4V is unstable at high temperature, and phase transformation from α phase to β phase happens at above phase-transition temperature during superplastic deformation [6–8]. Moreover, β phase is considered to be soft and has diffusivity 100 times higher than that of α phase, which affects the flow stress and the phase grain growth during the superplastic deformation. Thus the α/β ratio of Ti-6Al-4V decreases during the deformation. Not much attention has been given to understanding of β deformation characteristics and α/β phase rate effect on the deformation property since β phase exhibits large ductility in general and poses less difficulty in deforming process compared to α phase. Up to now, grain boundary sliding (GBS), diffusion creep and re-crystallization have been well accepted as the major mechanisms of superplastic deformation [7–10]. However, in the $\alpha + \beta$ phase Ti-6Al-4V, there are α phase, β phase, α/α phase boundary, α/β phase boundary and β/β phase boundary, how these phases and phase boundaries work and accommodate together is not clear. More efforts are needed to be done on these aspects.

Up to now, most of researchers have studied the superplasticity using constant strain rate method [6–9, 11, 12] and have found that the optimum strain rate can maintain the deformation in a more reasonable state and minimize the deformation time. In some occasions, instead of constant strain rate method, constant strain velocity method is used in the hot working operation, but this issue is studied rarely [13,14]. In this case, the strain rate is not constant, and rises with the tensile time due to the reduced cross-section area of the specimen.

*Corresponding author: Weidong Li, School of Mechanical Engineering and Automation, Beihang University, Beijing 100083, China, E-mail: space@buaa.edu.cn

Wei Guo: E-mail: gwei@buaa.edu.cn, Qiang Jia, Ruiting Li, School of Mechanical Engineering and Automation, Beihang University, Beijing 100083, China

In this work, the effects of deformation temperature and tensile velocity on the tensile force and elongation of Ti-6Al-4V titanium alloy sheets were investigated by constant velocity method. And the microstructure evolutions under various parameters (temperatures, tensile velocities and deformation strain) were analyzed to reveal the main deformation mechanism.

Experimental material and procedures

The material used in the present work was 2 mm thick Ti-6Al-4V sheet. The initial microstructure as shown in Figure 1 is typical $\alpha + \beta$ phase microstructure which consists of 93.65 % volume fraction primary α phase with the average grain size of 2.5 μm and 1.6 % volume fraction about 1.0 μm grain size secondary lamellar β phase.

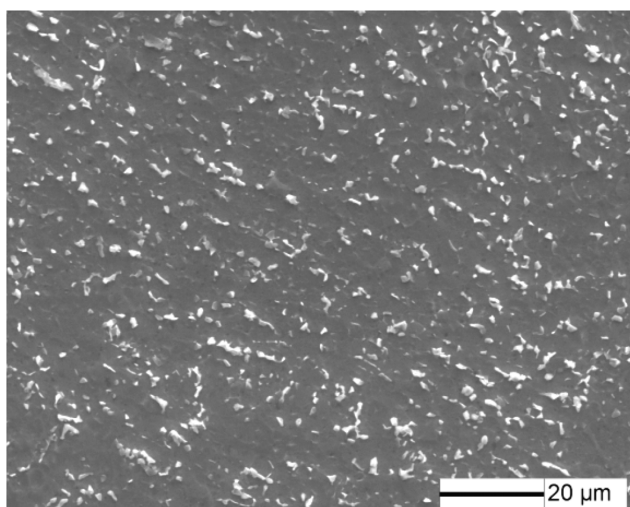


Figure 1: The microstructure of Ti-6Al-4V alloy.

The specimens with a gauge of 10 mm long and 8 mm wide were cut by wire-electrode cutting machine and machined to the dimensions of the tensile specimens are shown in Figure 2. Note that the tensile direction was parallel to prior-rolling direction of the sheet. The Electronic Universal Testing Machine was used to test the superplastic properties of Ti-6Al-4V alloy, and a furnace was attached to the machine, which can generate the temperature from room temperature to 1,100 °C.

Prior to test, Ti-6Al-4V specimens were coated by glass lubricant to prevent oxidation at higher temperature in air, and then were heated to the test temperature in furnace and hold the temperature for 6 min to ensure thermal

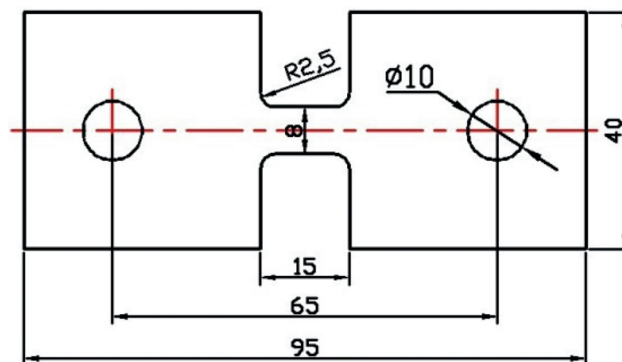


Figure 2: The dimensions of superplastic tensile specimen (mm).

equilibrium. The temperature of the specimen was monitored using a K-type thermocouples within $\pm 2^\circ\text{C}$ fluctuation inserted in the furnace. After superplastic tests, the specimens were water quenched immediately to keep the microstructures at the test temperature.

Tensile parameters of the superplastic deformation tests are listed in Tables 1 and 2. And the corresponding initial strain rate ranges from $5 \times 10^{-4} \text{ s}^{-1}$ to $1 \times 10^{-2} \text{ s}^{-1}$ based on the formula

$$\dot{\epsilon}_0 = v_0 / l_0 \quad (1)$$

Table 1: The tensile temperature parameters of the tensile tests.

Temperature (°C)	850	880	890	900	910	920	950
Velocity (mm/min)							0.6
Corresponding initial strain rate(s^{-1})							1×10^{-3}

Table 2: The tensile velocity parameters of the tensile tests.

Temperature (°C)	900 °C						
Velocity (mm/min)	0.3	0.4	0.6	0.9	1.2	3.0	6.0
Corresponding initial strain rate(s^{-1})	5×10^{-4}	6.7×10^{-4}	1×10^{-3}	1.5×10^{-3}	2×10^{-3}	5×10^{-3}	1×10^{-2}

where, $\dot{\epsilon}_0$ is the initial strain rate, v_0 is the tensile velocity, while l_0 means the initial gauge length of specimen. In the superplastic tensile experiment, the strain rate decreases continuously because of the elongation of the sample.

After superplastic tensile tests, the specimens were cut out from the tip of the fracture, mounted along longitudinal section with conductive powder, ground with a series of silicon carbide abrasive sheets, polished with

1 μm diamond paste followed by 0.05 μm alumina slurry, and etched with Kroll's reagent (3 ml HF, 6 ml HNO_3 and 100 ml H_2O). The microstructures and phase constituents of the specimen were evaluated by scanning electron microscope (SEM) typed CS3400 and transmission electron micrograph (TEM). The α or β phase grain sizes averaged from ten grains were evaluated by SEM.

Results and discussion

Superplasticity of specimens with various parameters

Figure 3 presents the maximum tensile force and the elongation of the specimens at various experimental temperatures. The maximum tensile force decreases as the temperature changes from 850 $^{\circ}\text{C}$ to 950 $^{\circ}\text{C}$ (Figure 3(a)). The maximum tensile force is about 0.5585 kN at 850 $^{\circ}\text{C}$ and the minimum value of 0.17 kN is attained at 950 $^{\circ}\text{C}$. It is reported that higher temperature leads to greater thermal activation, which can decrease the critical shear stress, enhance atom free energy, and improve the ability of grain boundary sliding and diffusion creep [15]. In addition, softening effect caused by dynamic-recover and re-crystallization becomes greater as the temperature

increases [16]. Thus, the decrease of tensile force occurs as the temperature increases. It is noted that the elongations of all specimens at various temperature exceed 600 % (shown in Figure 3(b)). From 850 $^{\circ}\text{C}$ to 900 $^{\circ}\text{C}$, increasing temperature leads to higher elongation, and the highest elongation of 1220.5 % is observed at 900 $^{\circ}\text{C}$. When the temperature exceeds 900 $^{\circ}\text{C}$, the elongation of specimen decreases with the temperature rising. When the deformed temperature is 950 $^{\circ}\text{C}$, the elongation decreases to about 700 %.

Figure 4 shows the maximum tensile forces and the elongations of the specimens at various tensile velocities. It can be seen that the maximum tensile force increases as the tensile velocity increases in all experimental ranges (0.3 mm/min to 6 mm/min). With the increase of tensile velocity, the number of dislocation in Ti-6Al-4V titanium alloy increases rapidly and leads to the pile-up of dislocations. Strain hardening generated by dislocation movement and diffusion creep lead to the increase of the tensile force [15]. Thus the maximum tensile force increases with the tensile velocity. Note that the elongation of the specimen increases rapidly when the tensile velocity changes from 0.3 mm/min to 0.6 mm/min, and then decreases as the tensile velocity rises continuously. When the tensile velocity is 0.3 mm/min (low), the elongation is small (about 760 %). The effect of dynamic crystallization softening is comparably not obvious due

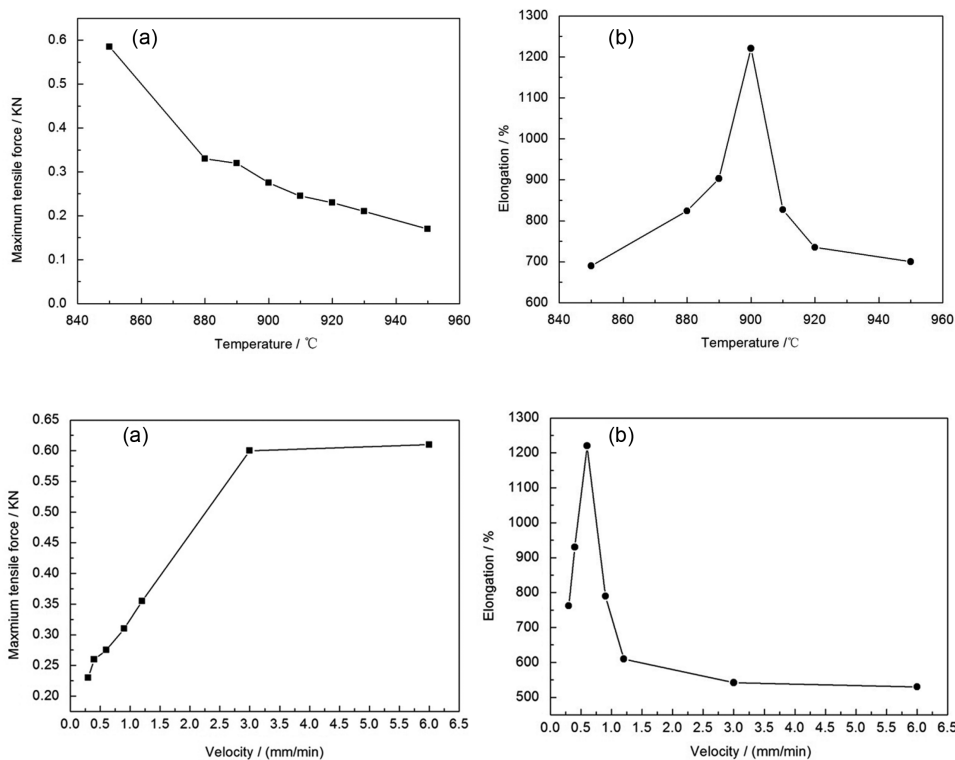


Figure 3: Temperature effect on the (a) maximum force and (b) elongation.

Figure 4: The tensile velocity effect on the (a) maximum force and (b) elongation.

to low strain energy during superplastic deformation [8]. Moreover, the grain size grows dramatically at very low deformation velocity (0.3 mm/min) owing to too long time maintaining at tensile temperature, which reduce the elongation. Thus the maximum elongation is attained at 0.6 mm/min tensile velocity. When the tensile velocity continually increases, the elongation decreases due to strain hardening. Specifically, when tensile velocity is 3 mm/min, the elongation of 542% is attained. This indicates that the tensile velocity plays an important role in the superplastic deformation process of TC4 alloy.

Microstructures of the superplastic deformation

Figure 5 shows the microstructures of the specimens in the temperature range of 850–950 °C at the tensile velocity of 0.6 mm/min. The equiaxed shape α and β phase grains are observed on the superplastic deformation specimens, which is the typical microstructural characteristics of superplastic deformation [17]. Since the basic material possesses very few equiaxed α grains, dynamic globularization of Ti-6Al-4V which influences the primary α grain size and grain size distribution occurs through

boundary splitting and thermal grooving [17,18]. Thus the equiaxed shape α and β phase grains are attained during the dynamic globularization process. In addition, α and β phase grain sizes increase gradually with the temperature rising. It is considered that the grain growth occurs due to not only the static grain growth but also the deformation enhanced grain growth [20]. On the other hand, the volume fraction (Vol%) of α phase decreases significantly, conversely lots of β phase grains emerge and grow into larger grains (Figure 5(a)–(d)) due to the fact that α phase changes to β phase at the temperature above phase transformation point. Higher temperature provides more energy for phase boundary migration, accelerates β phase to swallow small grains around, so β phase increases with the temperature rising. Figure 6 gives the data of α and β phase grain sizes and β phase volume fraction at various temperatures. It can be seen that at 850 °C, α and β phase grains are $\sim 4.5 \mu\text{m}$ and $\sim 2.5 \mu\text{m}$ respectively (small). And β phase volume fraction is about 5.26 %, which is small but a little larger than that of basic material (1.6 Vol%). Note that the diffusivity of β phase is about two orders of magnitude higher than that of α phase [21], thus β phase grows faster than α phase. As the temperature changes from 850 °C to 900 °C, both α and β phase grains grow but β phase grain grows faster,

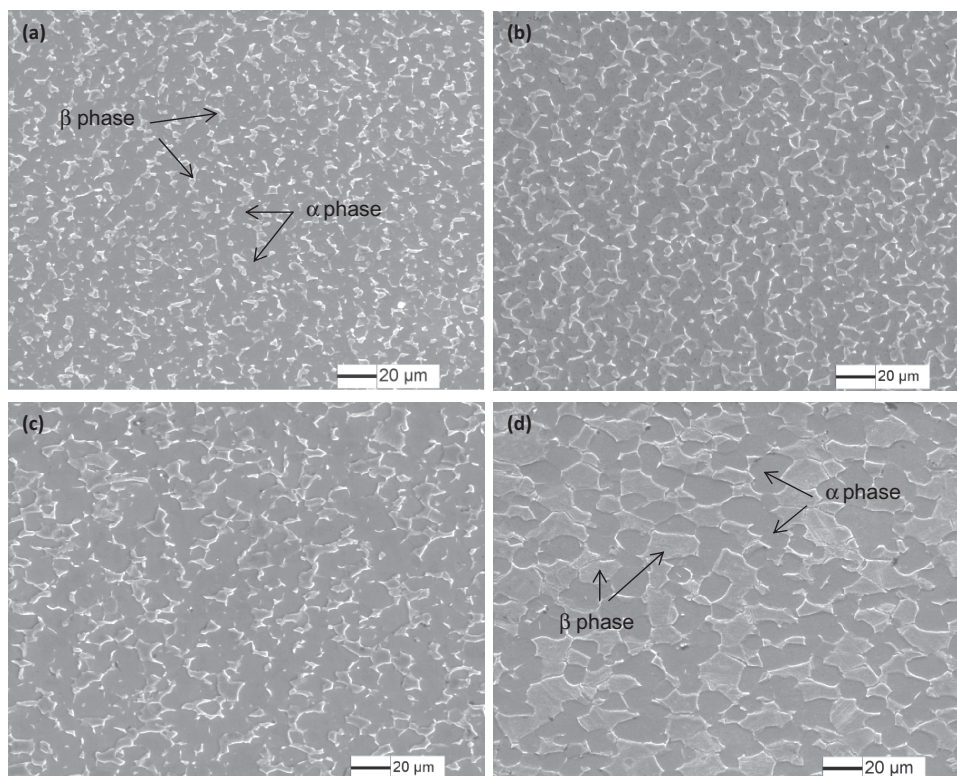


Figure 5: The microstructures of the specimens in the temperature range of 850–950 °C (a) 850 °C, (b) 880 °C, (c) 900 °C, (d) 950 °C.

i. e., β phase volume fraction increases gradually. The best elongation is attained under the condition of $\sim 7.0\ \mu\text{m}$ α phase and $\sim 4.0\ \mu\text{m}$ β phase and the β phase volume fraction is about 31%. When the temperature reaches $950\ ^\circ\text{C}$, more coarsening phase grains ($\sim 9.1\ \mu\text{m}$ α phase and $\sim 9.7\ \mu\text{m}$ β phase) are attained (Figure 6) and β phase volume fraction is about 57%, the elongation is reduced to 700 %.

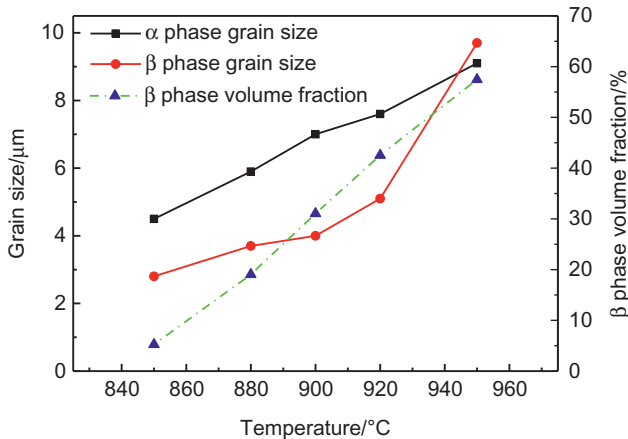


Figure 6: The phase grain sizes and β phase volume fraction of specimens at various temperatures.

In summary, when the temperature changes from $850\ ^\circ\text{C}$ to $950\ ^\circ\text{C}$, the microstructure of the specimens is changed in two aspects. One is that α and β phase grains grow with the temperature, and the other is that β phase volume fraction increases with the temperature. The growth of α and β phase grains is the main possible reason of decrease of the maximum tensile force during superplastic deformation. Since β phase (Body Centered Cubic, b.c.c.) owns lower flow force at higher temperature due to its abundant slip system than α phase (Hexagonal Close-Packed, h.c.p.) [21], thus the increase of β phase fraction is of benefit to the decrease of the maximum tensile force. For elongation, β phase fraction has obvious effect on its superplasticity from the experimental data (Figures 3 and 6). The elongation of the specimen increases with the increase of β phase fraction at first stage (from $850\ ^\circ\text{C}$ to $900\ ^\circ\text{C}$), which shows β phase fraction increase improves the superplasticity of TC4 alloy. Note that the α/β and β/β boundaries increase and α/α boundary decreases with the β phase fraction increase, thus the superplastic deforming ability increases owing to the contribution of α/β boundary sliding [10]. When the volume β phase fraction reaches about 31% ($900\ ^\circ\text{C}$), the superplasticity of Ti-6Al-4V reaches the highest value (Figure 3(b)). However, the increase of β volume fraction

can also induce microstructural changes associated with static and dynamic grain over-growth at high temperature, which leads to the deterioration of superplasticity. When the temperature is $950\ ^\circ\text{C}$, 57 Vol% β phase is attained. However, too higher β phase volume fraction leads to decrease of the elongation shown in Figure 3(b).

Figure 7 shows the microstructures of specimens with various tensile velocities at $900\ ^\circ\text{C}$. When the tensile velocity is high (3.0 mm/min and 1.2 mm/min), the phase grains are relatively finer but even bigger than original phase grains, as shown in Figure 7(a) and (b). When the tensile velocity is low (0.3–0.6 mm/min), the phase grains become coarser obviously due to grain growth as mentioned above (Figure 7(c) and (d)). Figure 8 gives α and β phase grain sizes of the specimens with the various tensile velocities. It can be seen that α and β phase grains decrease with the increase of the tensile velocity. Note that the amount of deformation is one of important conditions for the occurrence of recrystallization [22]. The larger velocity of deformation, the larger the driving force of recrystallization and less time for grains to grow. Thus, stress concentration cannot be released timely and strain energy is large enough for sufficient dynamic recrystallization at higher velocity, and the phase grain is comparable finer.

To investigate the superplastic deformation mechanisms and its accommodation, the microstructures of deformation specimens are observed by TEM, shown in Figure 9. Planar arrays of dislocations are discovered on α phase and α/α phase boundary in the microstructure of specimen at $850\ ^\circ\text{C}$ and 0.6 mm/min (Figure 9(a)), indicating that grain boundary sliding (GBS) at the α/α phase boundary and the grain matrix deformation in α phase grain happen during superplastic deformation. However, note that there is only about 5.26 Vol% β phase at the condition of $850\ ^\circ\text{C}$ and 0.6 mm/min (shown in Figure 6), lots of α/α phase boundaries and less α/β phase boundaries exist in the microstructures. The harder α phase acts as a skeleton which undergoes virtually the entire applied load and dominates the deformation behavior [10]. At $900\ ^\circ\text{C}$ and 0.6 mm/min condition, glide steps at α/α and α/β phase boundaries can be observed, shown in Figure 9(b). Note that dislocations inside α phase grain are also visible. It also can be seen that the α/α grain boundaries maintain clear and straight lines after deformation, but α/β boundary is curved and indistinct, indicating that phase boundary sliding occurs predominantly at α/β boundary, and α/β boundary makes more contribution than α/α phase boundary does due to the fact that the sliding resistance increases on the order

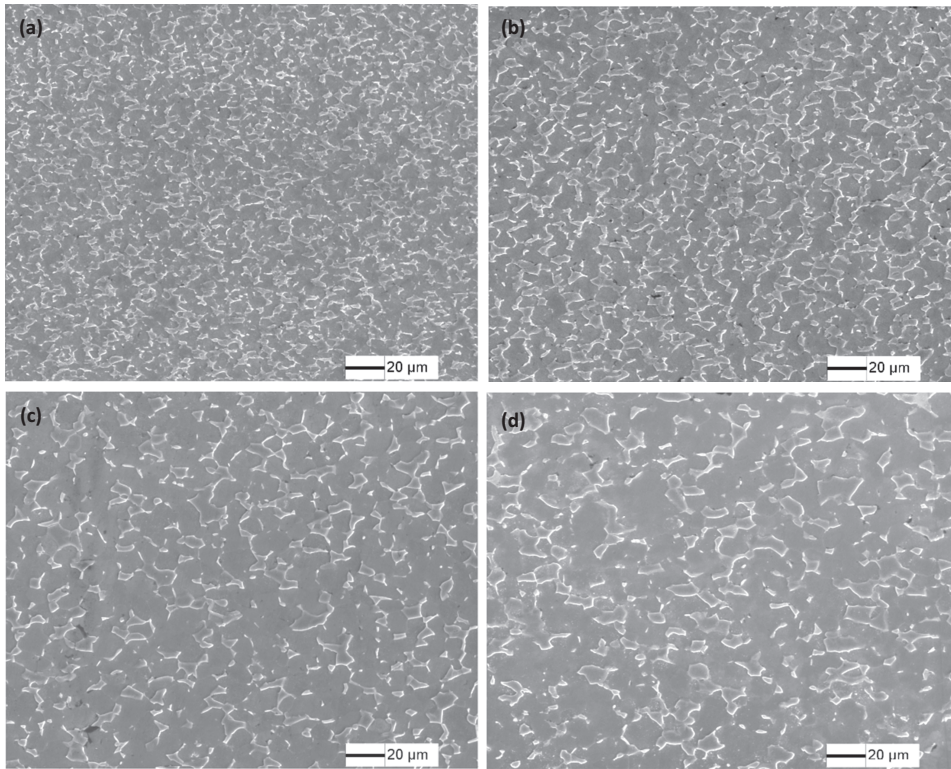


Figure 7: Ti-6Al-4V microstructures near fracture surface after hot tensile deformation (a) 3.0 mm/min, (b) 1.2 mm/min, (c) 0.6 mm/min, (d) 0.3 mm/min.

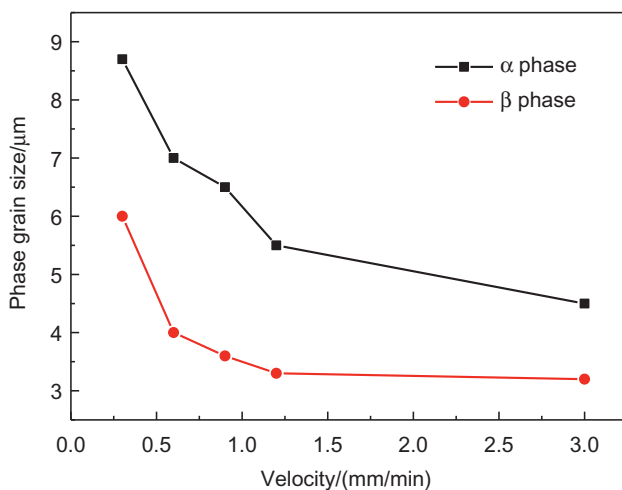


Figure 8: The phase grain sizes of specimen at various deformed velocities.

of $\alpha/\beta < \alpha/\alpha \approx \beta/\beta$ [10]. Note that the volume fraction of β phase is about 31% under the condition of 900 °C and 0.6 mm/min deformation condition, and the α phase skeleton can be broken by softer β phase as low as 26 Vol% [10], and β phase is the dominant factor in the superplastic deformation now [23,24].

Microstructures of various positions of superplastic deformation specimen

The microstructures at various positions of superplastic deformation Ti-6Al-4V under the optimum tensile parameter (900 °C, 0.6 mm/min) have been studied. How the specimens are cut from the deformation specimen is shown in Figure 10. In the gauge section, the tensile strain continuously increases from gripping head region (Figure 10(d part)) to the fracture tip region (Figure 10(d part)).

The longitudinal section microstructures of various positions are shown in Figure 11. Grain growth comparing with that of basic material (Figure 1) is observed at the gripping head (Figure 11(a)). It is mentioned that the gripping head section is usually considered only statically annealed without any effect of deformation during the superplastic deformation test. Therefore the initial dynamic globularization process can be attributed exclusively to thermally activated process but not to any deformation process. From Figure 11(b) to (d), it can be seen that the phase grains grow up obviously as the tensile strain increases. It is noted that not only thermally activated processes but also the deformation strain process exist at

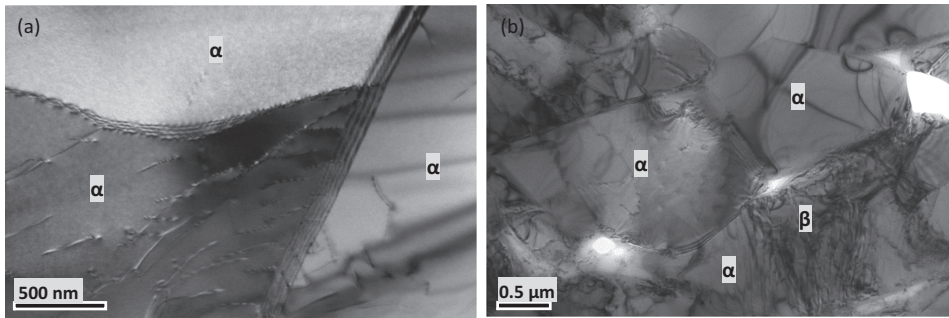


Figure 9: Transmission electron micrographs of superplastic deformed specimen (a) 850 °C (b) 900 °C.

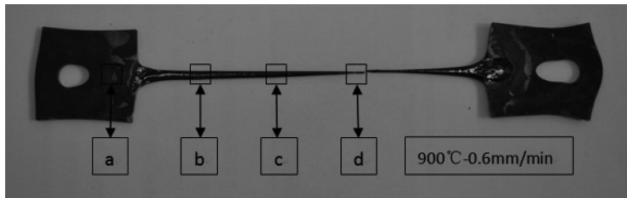


Figure 10: Various cutting points in the specimen.

the deformation regions (from Figure 10(b part) to Figure 10(d part)). Deformation strain accelerates grain growth (dynamic coarsening) has been proved to be one of the important microstructure characteristics during superplastic deformation [19, 25]. Furthermore, the deformation strain increases from near gripping region Figure 10(b part) to the fracture tip region (Figure 10(d part)). Thus the phase grain

grows faster from the gripping head region to the fracture tip region, which proved by the fact that the phase grain sizes increase at the same direction. In addition, it can be seen that β phase volume fraction increases from near gripping region (Figure 10(b part)) to the fracture tip region (Figure 10(d part)), as shown in Figure 11. This phenomenon indicates that dynamic grain growth and dynamic phase transformation accelerate the phase transformation from α phase to β phase [25].

Conclusions

The superplasticity of Ti-6Al-4V titanium alloy was evaluated by constant velocity tensile test in the temperature

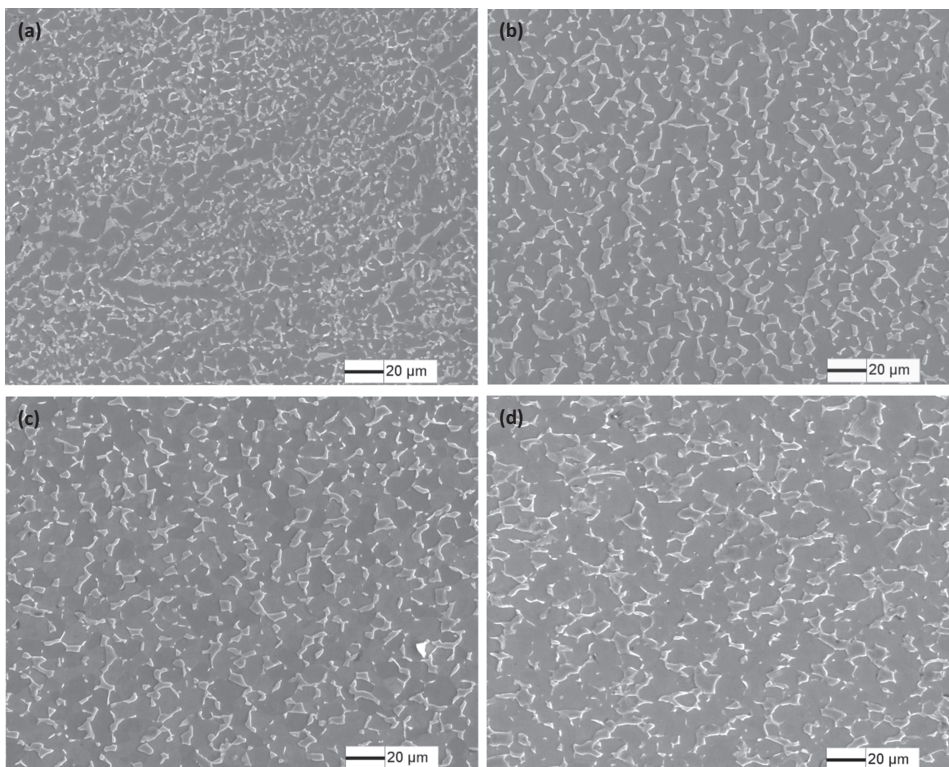


Figure 11: Microstructures at various positions of tensile specimen (a) a part (b) b part (c) c part (d) d part.

range of 850–950 °C. The deformation temperature, tensile velocity and deformation strain have obvious effects on the microstructure evolution of Ti-6Al-4V titanium alloy in following ways:

- 1) The maximum tensile force decreases from 0.5585 KN at 850 °C and the minimum value of 0.17 KN is attained at 950 °C. And much lower or higher temperature is not benefit to attain the optimum elongation due to pile-up of dislocations at low temperature and much growth of the phase grains at high temperature. The maximum elongation of 1220.5 % is attained under the condition of 900 °C and 0.6 mm/min. Furthermore, α phase and β phase grain sizes increase with the increase of the deformed temperature and decrease with the increase of the tensile velocity.
- 2) Grain growth and β phase transformation from α phase are the main phenomena during superplastic deformation. α and β phase grain sizes increase with the increase of temperature and decrease of tensile velocity. And β phase volume fraction of the tensile specimen increases with the increase of temperature, and β phase volume fraction plays an important role in superplasticity. The best elongation is attained under the condition of $\sim 7.0 \mu\text{m}$ α phase and $\sim 4.0 \mu\text{m}$ β phase and β phase volume fraction is about 31 %.
- 3) At the gripping head region, α phase and β phase grow only under only thermally activated process, and the phase grain sizes increase from the fracture tip region to gripping head region of deformation specimen due to larger deformation strain accelerating the grain growth.

Acknowledgements: This research was supported by International Science and Technology Cooperation Program of China (No.2013DFR50590), the fundamental Research Funds for the central University (No.30420100042, 3042012112 and 30420120771) and National Natural Science Foundation of China (No.50705050).

References

- [1] G. Wang, K.F. Zhang, D.Z. Wu, J.Z. Wang and Y.D. Yu, *J. Mater. Process. Technol.*, 178 (2006) 24–28.
- [2] Y.G. Zhou, W.D. Zeng and H.Q. Yu, *Mater. Sci. Eng., A*, 393 (2005) 204–212.
- [3] M. Vanderhastén, L. Rabet and B. Verlinden, *Mater. Des.*, 29 (2008) 1090–1098.
- [4] Y. Chen, K. Kibble, R. Hall and X. Huang, *Mater. Des.*, 22 (2001) 679–685.
- [5] C. Namas, *Int. J. NonLinear Mech.*, 37 (2002) 461–484.
- [6] A.V. Sergueeva, V.V. Stolyarov, R.Z. Valiev and A.K. Mukherjee, *Mater. Sci. Eng., A*, 323 (2002) 318–325.
- [7] R.Y. Lutfullin, A.A. Kruglov, R.V. Safiullin, M.K. Mukhametrakhimov and O.A. Rudenko, *Mater. Sci. Eng., A*, 503 (2009) 52–54.
- [8] S.D. Sun, Y.Y. Zong, D.B. Shan and B. Guo, *Trans. Nonferrous Met. Soc. China*, 20 (2010) 2181–2184.
- [9] G. Giuliano, *Mater. Des.*, 29 (2008) 1330–1333.
- [10] J.S. Kim, J.H. Kim, Y.T. Lee, C.G. Park and C.S. Lee, *Mater. Sci. Eng., A*, 263 (1999) 272–280.
- [11] A.V. Sergueeva, V.V. Stolyarov, R.Z. Valiev and A.K. Mukherjee, *Scr. Mater.*, 43 (2000) 819–824.
- [12] C.H. Park, Y.G. Ko, J.-W. Park and C.S. Lee, *Mater. Sci. Eng. A*, 496 (2008) 150–158.
- [13] A. Arieli and A. Rosen, *Scr. Metall.*, 10 (1976) 809–811.
- [14] M.L. Guo, 11th International Conference on Technology of Plasticity, ICTP 2014, October, 19–24, 2014, Nagoya Congress Center, Nagoya, Japan (2014), 1090–1095.
- [15] D.H. Cheng, J.H. Huang, J. Yang, H. Zhang and J. Rare, *J. Rare. Met. Mater. Eng.*, 39 (2010) 277–280 (in Chinese).
- [16] P. Honarmandi and M. Aghaie-Khafri, *Metallogr. Metallogr. Microstruct. Anal.*, 2 (2013) 13–20.
- [17] T.G. Nieh and J. Wadsworth, *Mater. Sci. Eng., A*, 239–240 (1997) 88–96.
- [18] S. Roy and S. Suwas, *J. Alloys Compd.*, 548 (2013) 110–125.
- [19] S. Roy and S. Suwas, *Mater. Des.*, 58 (2014) 52–64.
- [20] D.S. Wilkinson and C.H. Cáceres, *Acta Metall.*, 32 (1984) 1335–1345.
- [21] M.L. Meier, D.R. Lesuer and A.K. Mukherjee, *Mater. Sci. Eng. A*, 136 (1991) 71–78.
- [22] T. Seshacharyulu, S.C. Medeiros, W.G. Frazier and Y.V.R.K. Prasad, *Mater. Sci. Eng. A*, 284 (2000) 184–194.
- [23] P.G. Partridge, D.S. McDermid and A.W. Bowen, *Acta Metall.*, 33 (1985) 571–577.
- [24] J.A. Wert and N.E. Paton, *Metall. Trans. A*, 14 (1983) 2535–2544.
- [25] L.J. Huang, L. Geng, P.Q. Zheng, A.B. Li and X.P. Cui, *Mater. Des.*, 30 (2009) 838–841.